UDC 634.7:612.858.4

SH. TAKEDA,[1–3] P. MANNSTRÖM,[1] S. DASH-WAGH,[1] T. YOSHIDA,[2] and M. ULFENDAHL[1]

EFFECTS OF AGING AND NOISE EXPOSURE ON AUDITORY BRAINSTEM RESPONSES AND NUMBER OF PRESYNAPTIC RIBBONS IN INNER HAIR CELLS OF C57BL/6J MICE

Received April 20, 2016

C57BL/6J mice develop age-related hearing loss (HL) early in life. The influence of aging and noise exposure on the number of presynaptic structures in inner hair cells of C57BL/6J mice has not been studied. We monitored auditory brainstem responses, ABRs, in C57BL/6J mice over time and assessed changes in the number of inner hair cell presynaptic ribbons. Multifaceted verification of the effects of aging and noise exposure on hearing in the C57BL/6J strain was performed. The HL was additively increased by noise exposure in 5-week-old mice. The earliest change observed was a decrease in the amplitude of the ABR first wave. Hair cells and spiral ganglion neurons were also lost. Immunohistochemistry and high-resolution confocal microscopy revealed decreased numbers of CtBP2-positive structures in the inner hair cells localized in other than those in the low-frequency region of the cochlea. On the other hand, the influence of acute noise exposure on the inner hair cell ribbons was observed only within the highest-frequency area.

Keywords: auditory brainstem response, C57, cochlear synaptopathy, CtBP2, hearing loss, inner hair cell ribbons.

INTRODUCTION

The elderly population has increased within recent years, and, therewith, presbycusis has become a significant social problem [1, 2]. Although hearing impairment might be due to multiple factors, noise exposure is reported to be a key contributor [3, 4].

The C57BL/6J mouse strain exhibits progressive hearing loss, which begins from high frequencies, similar to human presbycusis [5–10], and these mice are susceptible to acoustic overstimulation [11, 12]. Thus, this strain has been considered to be a suitable model of age-related hearing loss (AR HL) and noise-induced hearing loss (NI HL). Genetic analysis showed that the HL in the C57BL/6 strain is inherited as a recessive trait [13]. The genetic defect was revealed as a splice variant of the gene encoding cadherin 23 [14], a component of the stereocilia tip links that are necessary for hair cell (HC) mechanotransduction [15]. Synaptic structures and peripheral innervation patterns are normal in immature and young adult C57 mice, but progressive HL characteristic of the C57 mice has been suggested to be associated with innervation of inner hair cells (IHCs) [16].

Age-related declines differ between the C57BL/6J and CBA/CaJ mouse strains and humans, while normalizing for the difference in the mean lifespan and frequency range. It was observed that threshold elevation and neural loss were apparently more severe for the C57BL/6J strain than for the other mouse strains and for humans. Additionally, besides the profound HL at high frequencies, C57BL/6J mice exhibit the respective HL, although less severe in its magnitude, at low frequencies [17–19].

Auditory nerve fibers carry information from the IHCs of the cochlea to the brain. Each auditory nerve fiber makes a synaptic contact with a single IHC [20]. The number of IHC ribbons (presynaptic structures) reduces with age in CBA/CaJ mice [21]. The noise-induced reduction in IHC ribbon numbers has also been reported in the guinea pig [22]. Disruption of the synaptic connections to IHCs and glutamate excitotoxicity and/or a complex accumulation of these

[1] Department of Neuroscience, Karolinska Institutet, Stockholm, Sweden.
[2] Department of Otolaryngology, Ehime University Graduate School of Medicine, Ehime, Japan.
[3] Oiki Ear and Nose Surgicenter, Osaka, Japan.
Correspondence should be addressed to Sh. Takeda (e-mail: rbjmk092@ybb.ne.jp).

factors with morphological changes have been reported [23, 24]. Electron microscopic studies revealed that degeneration progresses from the synaptic terminal, through the peripheral axon, to the cell body [25]. However, the influence of aging on the presynaptic structures combined with the effect of noise exposure has only been reported for the CBA/CaJ mouse and the guinea pig, while that for the C57BL/6J mouse strain has not been studied. C57BL/6J mice represent a popular animal model and have several features useful for the study of HL, as described above.

Here, we monitored auditory brainstem responses (ABRs) in C57BL/6J mice over time and assessed changes in hair cells and presynaptic ribbons in response to aging and noise exposure.

METHODS

A total of 29 female C57BL/6J mice (RRID: MGI_2677878) were obtained from the Charles River Laboratory (Sulzfeld, Germany) at the age of 3–4 weeks. In this study, we selected females, as aged female C57BL/6J mice have been reported to show significantly more severe HL (Willott et al, 2008 [35]). Mice were acclimated to their new surroundings for 7 days before testing commenced. The animals were housed in a temperature- and humidity-controlled vivarium under a 12-h light/dark cycle, and all animals were tested during the light phase. Mice were allowed free access to chow (Harlan Teklad TD120792, Sweden) and water. The diet was continued until the mice were sacrificed at the age of 36 weeks.

Animal Groups. Mice were randomly divided into three groups, young (Y; n = 10), non-noise exposure (Non-NE; n = 9), and noise exposure (NE; n = 10). The ABR thresholds were measured in all animals using ABR testing at 4 weeks of age. Mice in the Y group were sacrificed immediately after the ABR measurement. A mark indicating a number was applied to the pinna of Non-NE and NE groups, so that ABR measurements were performed blindly, and mice of both groups received similar treatment and were kept in a similar environment. The NE group was exposed to noise at 5 weeks of age, and the hearing thresholds were measured on the following day. After that, the ABRs of the Non-NE and NE groups of mice were measured at 6, 8, 12, 16, 20, 24, 28, 32, and 36 weeks of age. All these animals were sacrificed after the final ABR measurement, and histological examination was performed.

ABR Measurement. Auditory function was assessed by recording sound-evoked ABRs. Animals were anesthetized via i.p. injection of ketamine (100 mg/kg) and xylazine (10 mg/kg). Frequency-specific tone bursts of 3.5, 7, 14, 28, and 32 kHz were generated at durations of 2, 1, 0.5, 0.25, and 0.125 msec for the respectively frequencies and with a 1-msec raise and fall phases by means of a TDT system II (BioSig 32, Ver 3.12, Tucker Davis Technologies, USA). The tone bursts were presented through an electrostatic speaker (EC1, Tucker-Davies Technologies), with an earphone placed in the left ear canal of the anesthetized animal. Three sub-dermal needle electrodes were placed at the vertex (active), behind the left ear (reference), and in the left hindlimb (earth), respectively. Difference potentials were amplified and displayed as waveforms in the BioSig RZ software program (Tucker Davis Technologies). The first peak of the potential was used as the reference peak (henceforth referred to as wave 1). The intensity of the tone burst was decreased from 90 dB by 5-dB sound pressure level (SPL) decrements until the waveform disappeared. The lowest presented stimulus that elicited a reproducible response by visual inspection of stacked waveforms, after 1000 averages, was reported as the threshold. The amplitudes (wave-1 peak to the subsequent component) and latency times (time from the beginning of the stimulus to the wave-1 peak) were measured by off-line analysis of the stored waveforms.

Noise Exposure. To induce a permanent threshold shift (PTS), the NE group was exposed to an intense low-frequency noise (narrow band-free field noise, 0.8-7.2 kHz, at 110 dB SPL, for 4 h) at 5 weeks of age. The noise exposure was carried out in a soundproof box with a Beyma TD-360 horn (Acustica Beyma, Spain) attached to the ceiling of the box (centrally positioned inside the box, 85 cm above the animal cages). The noise was generated using 3560-C PULSE hardware and a LAB 300 amplifier with PULSE LabShop Version 13.1.0.246 software (Brüel and Kjær, Denmark). A microphone was placed centrally at the same level as the cages and used for adjusting the intensity level of the noise to less than 1 dB variation.

Histological Preparation and Assessment. Following the final ABR measurement, anesthetized animals were perfused intracardially with 4% paraformaldehyde in 0.1 M phosphate-buffered saline (PBS). After perfusion, both cochleae were removed, and the round and oval windows were opened.

Estimation of Cell Numbers and Volumes. All right-side cochleae from the three groups were immersed with a fixative containing 2.5% glutaraldehyde in PBS, followed by decalcification in 0.1 M ethylenediamine tetraacetic acid (EDTA) for about 72 h. After decalcification, the cochleae were post-fixed with 1% osmium tetroxide, dehydrated, and infiltrated and embedded in a 2-hydroxyethyl metacrylate-based resin (Technovit 7100, Heraeus, Germany). Serial sections (20-μm-thick) from the whole cochlea were stained with hematoxylin and eosin.

The method we used to estimate the cell numbers and volume of tissue specimens has been reported previously [26–29]; it is appropriate for evaluation of the components of the organ of Corti [30]. By applying the Cavalieri principle [31] and optical fractionator technique [32], total numbers of IHCs, outer hair cells (OHCs), and total numbers and soma cell volumes of spiral ganglion neurons (SGNs) were also estimated in each cochlea. For this procedure, a microscope (Axioplan, Zeiss, Germany) with a motorized stage and an electronic microcator (Prior ProScan II) with digital readout for measuring movements in the Z-direction was interfaced with a digital camera (Pixel link) and a personal computer-running newCAST software (Visiopharm, Denmark) that randomly places counting grids over the live image of sections (a newCAST web) was used. The procedure used to estimate the total number of cells using newCAST software has been previously described [30]; a counting frame was randomly placed over a section at ×100 magnification by newCAST software. All IHCs and OHCs, as well as SGNs, were counted manually within the frame. Neurons were concurrently assessed to establish the cell soma volume using the nucleator technique, where the average distance from the most centrally placed nucleolus to the cell membrane were calculated in four randomly placed test lines per neuron.

Counting CtBP2 Positive Presynaptic Ribbons. The left-side cochleae from all three groups were immersed with a fixative containing 4% paraformaldehyde in PBS for more than 6 h. They were transferred to a fresh dish, and the surrounding bone was gently removed using sharp tweezers and microscissors. The entire lateral walls of the cochlear capsule were opened with minimum damage to the organ of Corti. The organ of Corti was microdissected into five pieces (dissected into ca. half-turns). After rinsing in PBS, the specimens were permeabilized in 0.3% Triton X-100 in PBS for 20 min at room temperature, blocked in a solution of 5% goat serum in 1% bovine serum albumin in PBS for 1 h, and incubated overnight at 4°C in the primary antibodies (mouse anti-CtBP2 [1:400, BD Biosciences, USA, RRID:AB_399431] and rabbit anti-myosin-VIIa [1:400, Proteus Biosciences, USA, RRID:AB_10015251]). After washing in PBS, the samples were incubated with species-appropriate secondary antibodies for 60 min at room temperature. A frequency-place map for the C57BL strain [33, 34] was used to identify cochlear regions for counting IHCs and ribbon synapses.

The nuclei of the IHCs and OHCs were stained with anti-CtBP2 antibody; we confirmed cochlear regions, identified the respective frequency areas under a confocal microscope, and counted CtBP2-positive presynaptic ribbons. Confocal Z-stacks were obtained of the IHCs at the 3.5, 7, 14, 28, and 32 kHz regions of each cochlea (LSM510; Carl Zeiss, Germany) using a high-resolution oil-immersion objective (alpha Plan-Fluar ×100/1.45) with digital zoom. Each region was observed from the endolymphatic surface of the organ of Corti; images in both X and Y planes were set to 112.28 μm. Furthermore, Z-slice images were taken in steps of 0.332 μm, so that each stack contained the entire vertical extent of about 10 IHCs (Z-depth was set to about 50 μm). A total of 150 pictures were taken at a 50-μm Z depth and were reconstructed for counting.

Statistical Analysis. Values are presented below as means ± s.d. First, data distributions were tested for normality using the Shapiro–Wilk normality test. When distributions were not normal, the Mann–Whitney U test was used. For parametric statistical analysis, one-way ANOVA followed by the Holm method was used. Statistical analysis was performed using EZR (Saitama Medical Center Jichi Medical University http://www.jichi.ac.jp/ saitama-sct/SaitamaHP.files/statmed.html); P values <0.05 were considered to be statistically significant.

For the estimated cell numbers, total variation (CVtotal = s.d./mean) was calculated for each of the values of the stereological estimation. The total variation in the estimate depends on both error variance of the method (CVmethod) and biological variation between animals. The relation can be described using the following formula: $[CVtotal]^2 = [CVmethod]^2 + [CVbiol]^2$. The stereological sampling design was such that the variance error of

the method was below 0.5. The SigmaPlot statistical package (Version 11.0, Systat Software, Inc., USA) was used for all statistical computations.

RESULTS

Experimental Paradigm. The ABRs were measured for all animals at 4 weeks of age. For the NE group, the noise exposure was induced at 5 weeks of age. The ABRs were measured over time in both Non-NE and NE groups blindly. Histological evaluations were performed at 4 weeks of age in the Y group, and at 36 weeks of age in the Non-NE and NE groups.

Sequential Changes in the ABR Threshold, Amplitude, and Latency Time. There was no difference in the ABR thresholds between the groups at the first time point. The mean sequential ABR thresholds for the testing frequencies (3.5, 7, 14, 28, and 32 kHz) are presented in Fig. 1. All mice showed moderately high thresholds at 3.5 kHz from a young age, and an increase in this frequency due to aging was relatively small. For higher frequencies, on the other hand, the ABR thresholds were elevated markedly with increasing age. The mean thresholds of the Non-NE group at the age of 4 weeks were 51.7 ± 6.67 dB at 3.5 kHz and 17.2 ± 7.49 dB at 32 kHz. At the age of 36 weeks, the mean thresholds of the Non-NE group were 67.2 ± 12.0 dB at 3.5 kHz and 78.9 ± 25.2 dB at 32 kHz.

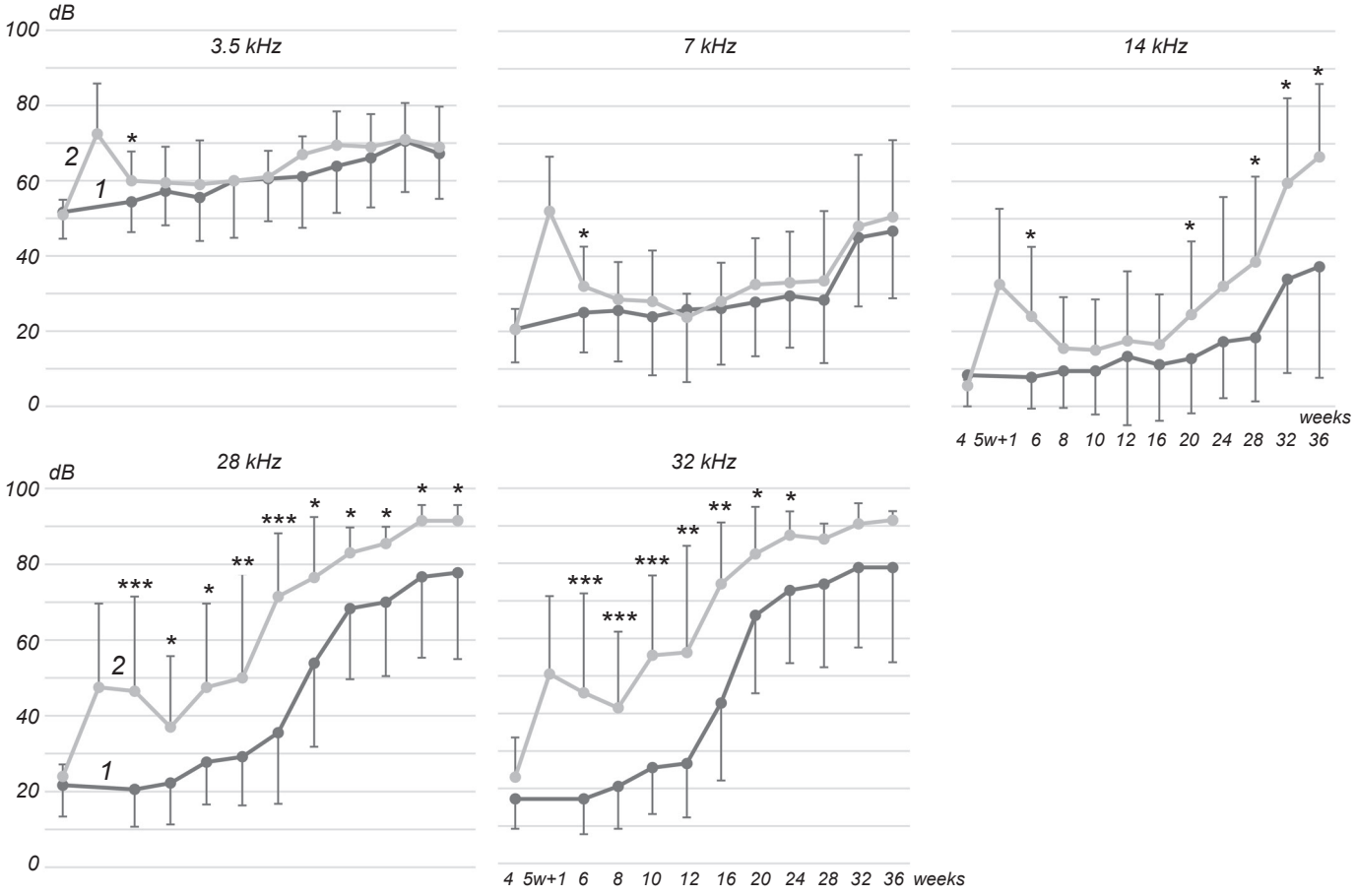

F i g. 1. Dynamics of the thresholds at each frequency (age, weeks, is shown below). The panels correspond to 3.5, 7, 14, 28, and 32 kHz (shown abowe). Graphs 1 correspond to Non-NE group. The NE group (2) was exposed to noise (broad-band, centered at 4 kHz with a span of 3.2 kHz, at a level of 110 dB SPL, for 4 h) at 5 weeks of age. Increases in the auditory brainstem response (ABR) threshold were especially severe at higher frequencies. The noise exposure caused both a transient threshold shift directly after exposure and continued to cause increased threshold shifts with age. At high frequencies in older animals, many of the individual thresholds reached the measurable limit of the equipment (90 dB). When the limit was exceeded, the threshold was defined as 95 dB. * $P < 0.05$, ** $P < 0.01$, *** $P < 0.005$ (Mann–Whitney U test).

Р и с. 1. Динаміка порогів для кожної з частот.

One day after noise exposure, the NE group showed a 20–30 dB increase in the thresholds at all frequencies. This threshold increase improved over time, but recovery was incomplete, especially at high frequencies. One week after noise exposure, the threshold remained significantly increased; *P* values for each frequency were: 0.0163 at 3.5 kHz, 0.0432 at 7 kHz, 0.0282 at 14 kHz, 0.00322 at 28 kHz, and 0.00153 at 32 kHz. The NE group showed significantly higher thresholds than those in the Non-NE group in a frequency- and age-dependent manner. The ABR thresholds at 14 kHz showed significant differences between the two groups at the ages of 6, 20, 28, 32, and 36 weeks; *P* values were 0.0282, 0.0355, 0.0153, 0.0444, and 0.0243, respectively. For thresholds at 28 kHz, the differences were significant at the age of 6–36 weeks (*P* values were 0.00322, 0.0122, 0.0306, 0.00721, 0.00459, 0.0192, 0.0286, 0.0148, 0.035, and 0.0296, respectively), whereas for 32 kHz, significantly different thresholds were obtained at 6–24 weeks of age (*P* values were 0.00153, 0.00246, 0.00181, 0.00524, 0.00646, 0.0188, and 0.016, respectively). As most of the ABR thresholds were higher than the measurable limit of the equipment for higher frequencies, i.e., 90 dB at older ages, the significance of differences was not calculated for the measurements from 32 kHz upwards at older ages. For the same reason, the slopes appear to reach a plateau at 28 and 32 kHz in mice at older ages.

Over time, with increasing age, the amplitudes of wave 1 tended to decrease in both NE and Non-NE groups (Fig. 2). A reduction in the amplitude

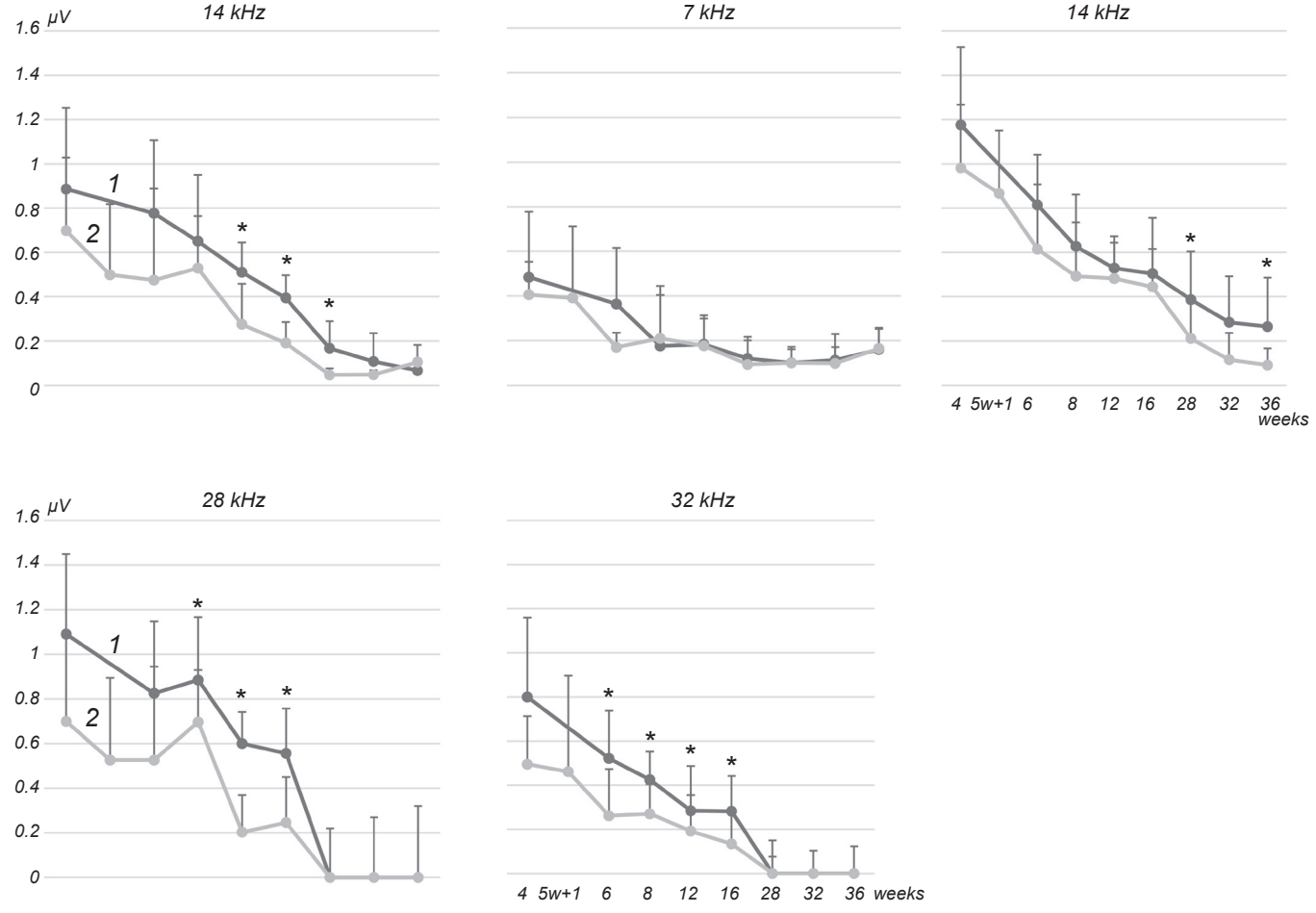

F i g. 2. Mean auditory brainstem response (ABR) amplitudes of wave 1 elicited by tone burst stimuli. As age advanced, the ABR wave 1 amplitudes decreased in both Non-NE and NE groups. The number of old animals was not sufficient for statistical analysis of higher-frequency (28 and 32 kHz) values, as many of the animals failed to respond at 80 dB stimulation. * $P < 0.05$ (Mann–Whitney *U* test). Other designations are similar to those in Fig.1.

Р и с. 2. Середні значення амплітуди хвилі I стовбурової слухової відповіді на дію тональних стимулів.

could already be noted at 32 kHz at 6 weeks of age, as compared to 4 weeks. The NE group showed significantly lower amplitudes than the Non-NE group, except at 7 kHz. At higher frequencies, the significance could not be calculated because the HL in both groups was too advanced.

The latencies of wave 1 were not significantly different between the two groups at any age (Fig. 3).

Cell Number and Volume Estimation in the Organ of Corti. The total number of IHCs and OHCs, as well as the number and mean volume of the SGNs, were estimated from histological sections of the right-side cochlea of all three groups (Table 1). We observed no differences in the SGN volume. The numbers of IHCs, OHCs, and SGNs were smaller in the Non-NE and NE groups as compared to the Y group. The cell numbers in the animals subjected to noise were reduced somewhat, but were not significantly different from those of the age-matched non-exposed animals.

Presynaptic Ribbons. We analyzed the IHC line in the Z-stacked images, and counted the number of presynaptic structures of the ribbon synapses (CtBP2-positive) for each IHC (Fig. 4). The average numbers of CtBP2-positive presynaptic structures at different frequencies are shown in Fig. 4B. In the Y group, there

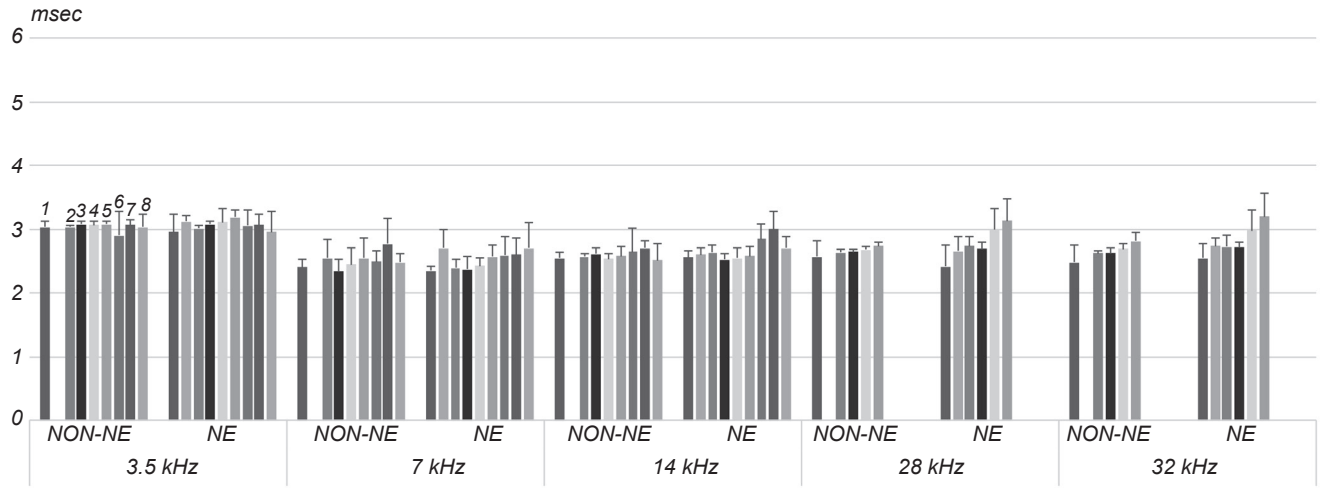

F i g. 3. Mean wave 1 latency times related to tone burst stimuli. With regard to the latency time, there was no significant change or difference either with aging or in response to noise. At high frequencies (28 and 32 kHz), aged waveform data were not available, because thresholds in aged animals often reached an overmeasuring limit.

Р и с. 3. Середні латентні періоди відповідей на дію тональних стимулів.

Table 1. Cell numbers and volumes

Таблиця 1. Кількість та об'єм клітин

Estimated cell numbers and volumes	Y, 4 weeks, untreated *n* = 8	Non-NE, 36 weeks *n* = 8	NE, 36 weeks *n* = 8
Total number of HCs	3207 ± 595	2072 ± 518 ***	1732 ± 241 ***
That of IHCs	731 ± 197	517 ± 79 **	464 ± 83 ***
That of OHCs	2376 ± 441	1555 ± 455 ***	1268 ± 190 ***
Total number of SGNs	14595 ± 1517	12888 ± 1303	2308 ± 1945 *
Volume of SGN (μm^3)	2339 ± 444	2267 ± 701	2241 ± 402

F o o t n o t e s. HCs are hair cells, IHCs – inner hair cells, OHCs – outer hair cells, and SGNs – spiral ganglion neurons. *P = 0.01, ** P = 0.004, ***P < 0.001 (one-way ANOVA + Holm–Sidak *post-hoc* test, compared with the Y group)

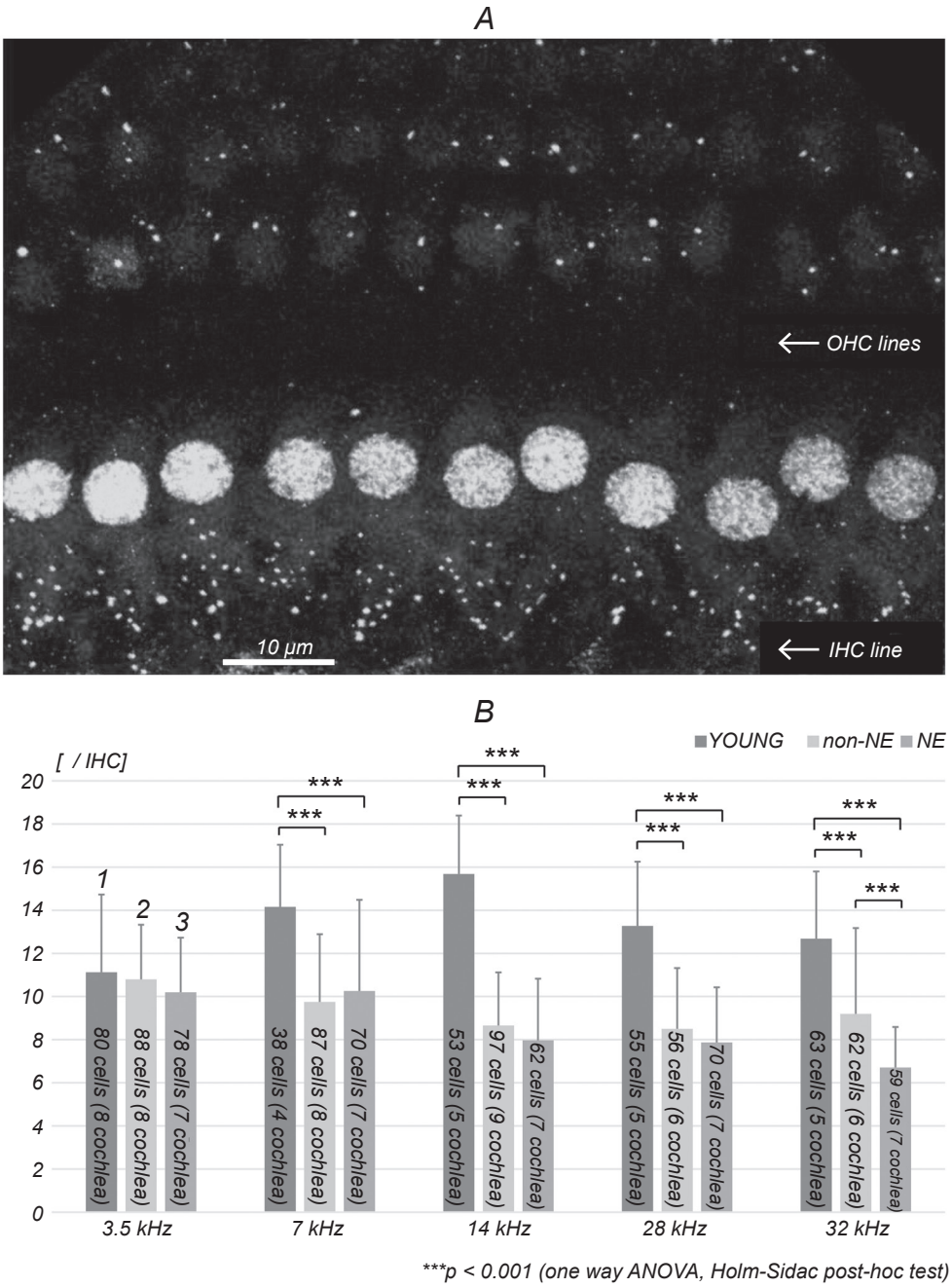

F i g. 4. A) Confocal Z-stacks of the hair cell region. A representative image of the hair cell region with a focus on the inner hair cells (IHCs). Cell nuclei and ribbon synapses were immunostained for CtBP2 (green), and the cytoplasm of the hair cells were immunostained for myosin VII (blue). About 10 IHCs were included in one field of view. B) Number of ribbon synapses per IHC is displayed for different groups (Y, Non-NE, and NE) at different parts of the cochlea, with respect to the hearing frequencies (3.5. 7, 14, 28, and 32 kHz). The number of ribbon synapses in older animals was significantly smaller. In high-frequency regions, the NE group showed significantly fewer synapses than the Non-NE group. ***$P < 0.001$ (one way ANOVA, Holm–Sidac *post-hoc* test).

Р и с. 4. Конфокальні Z-стеки для регіону волоскових клітин (*А*) та кількість стрічкових синапсів на волоскову клітину в різних групах (Y, Non-NE та NE) та різних частинах завитка (щодо слухових частот, 3.5, 7, 14, 28 та 32 кГц; *Б*).

were 10-15 such structures for each IHC. This number was significantly reduced with aging, except for the 3.5-kHz region. There was a significant difference between the Non-NE and NE groups only in the 32-kHz region, corresponding to the basal part of the cochlea.

DISCUSSION

There have been a number of reports about hearing and HC loss in the C57BL/6J mice strain. Hequembourg et al. examined the ABR thresholds of mice from 1.5 to 15 months of age, while Willott et al. examined mice from 1.5 to 9 months of age, and both reported high ABR thresholds for low frequencies, from a young age, as well as progressing age-related HL, which was more severe at high frequencies [19, 35]. Although demonstrating slow progression and a moderate severity, the CBA strain has also been reported to demonstrate a similar pattern of changes in the hearing sensitivity [36]. Noise exposure induced a marked threshold shift in the NE group, which partly recovered up to 2 weeks after the noise exposure. For higher frequencies, the NE animals showed a threshold shift that was 20-30 dB higher than that in the non-exposed animals, and this remained as the animals aged.

Wave 1 represents mostly the summed activity of the cochlear nerve [37]. Its amplitude generally corresponds to the strength of the neuronal signal, i.e., neurons responding synchronously to the stimulus onset. We observed that these amplitudes were reduced with aging, and this was further exacerbated by noise exposure. This suggests that synaptic dysfunction or neuropathy occurs due to both aging and noise exposure. Similar findings have been reported using an aging model in CBA/CaJ mice [21, 38]. The mechanism has been presumed to involve a reduction or dysfunction in the synaptic structure, rather than neuronal demyelination, as a disorder of electrosaltatory transmission would be reflected in a significantly prolonged latency [39]. This suggests that the genetic abnormality of the C57BL/6J strain does not cause increases in the latency, at least not within the high-frequency range [14, 15].

The software used for stereological analysis in our study allowed calculation of the volume of structures and cells and the total number of cells throughout the cochlea, from its base to the apex. Stereological analysis showed that the total number of IHCs and OHCs was significantly smaller in the aged mouse groups. While we could not obtain a complete cochleogram in this study, at least until 36 weeks of age, most of the missing HCs were observed in previous reports to affect the area more than 80% distant from the apex [19, 35]. In our study, the cell numbers in NE animals were reduced, but there were no statistically significantly differences from those of the age-matched Non-NE animals.

More than 80% of SGNs were maintained in both aged mouse groups; a significant difference was observed only between the Y group and the NE group. The SGN cell body loss in the basal turn of the cochlea has been suggested to reflect a latter mechanism than HC loss [19]; this was consistent with previous reports about the phenomenon of secondary neural degeneration that occurs subsequent to HC loss after noise exposure [40–43].

Using CtBP2 staining, we examined the average number of presynaptic ribbons per IHC within each frequency range. Each ribbon synapse makes a contact with a single auditory neuron fiber [20, 44]. This noise-induced neuronal degeneration, which involves loss of synaptic terminals on IHCs, is observed at one day after noise exposure [38, 45]. In this study, CtBP2 counting was performed at 32 weeks after noise exposure. The orphaned ribbons have been reported to be less than 10% in both young and aged mice [21, 22]. Thus, the number of presynaptic ribbons of an IHC reflects the numbers of remaining auditory nerve fibers. In the aged mouse groups, the number of ribbon synapses was noticeably reduced in the 7, 14, 28, and 32-kHz areas. Furthermore, this tendency was more notable within the higher-frequency range, but the number was not below half of the value of the Y group even at 32 kHz. A similar phenomenon has been reported in CBA mouse [21] and guinea pig [22]. Even when it occurred in the region showing the largest threshold shift in the oldest animals, the remaining number of ribbon synapses of the surviving IHCs was still half of that in young controls.

The auditory neuron fibers contacting each IHC has a specific spontaneous discharge rate (SR) and threshold for auditory stimulation, and these units are bimodally distributed according to their SR, i.e., high-SR (with a low threshold) and low-SR (with a high threshold) [46, 47]. It has been suggested that low-SR fibers are more vulnerable to acoustic trauma [22, 46] and aging [48]. This may be why significant decreases in the amplitude of wave 1 in both aged mouse groups in our study were observed before hearing thresholds shifted, even when the SGN decreases were small.

While the loss of low-SR fibers does not directly cause an increase in the ABR threshold, it has been reported to correlate with the amplitudes of wave 1 [49–51].

Changes in the ABR, loss of HCs and SGNs, and changes in the number of presynaptic ribbons due to aging in our study were similar to the findings reported earlier for other strains or species, despite the causal effect being a splice variant of the gene [14, 15]. Changes in the number of presynaptic ribbons due to noise exposure were, however, small, and significant differences were observed only in the 32-kHz region. In guinea pigs, ribbon loss has been reported in a more broad frequency range after noise exposure [22]. Along with genetic characterization of the C57BL/6J mouse, future detailed investigations are necessary. For example, the relationship between HL progression and the stability of the endocochlear potential (ECP) or tip links structure remains unclear [52]. Our study indicated the possibility that the C57BL/6J mouse has some tolerance to noise-induced synaptopathy.

Some limitations should be mentioned. In our study, we focused on the presynaptic structure of IHCs; we did not obtain DPOAEs or behavioral data, which would enhance the findings and have indicated an influence on the OHCs. Additionally, gender differences were not examined; it may be insightful to determine the effect of hormones on the results, to ensure that this did not bias our study. We could not obtain a full cochleogram or HC counts across all frequency ranges of the organ of Corti, as we used the right-side cochlea to determine cell numbers and estimate volumes and the left-side cochlea for counting CtBP2-positive presynaptic ribbons. Due to certain technical difficulties in this study, we could not complete the HC counting from the same individuals; this should be addressed in future studies.

Acknowledgments. This work was supported by the Swedish Research Council (Grant No. 2010-7209) and, in part, by funding from the European Union Seventh Framework Programme (FP/2007-2013) under the grant agreement No 304925.

The skillful and generous support of colleagues of the Risling and Ulfendahl laboratories is gratefully acknowledged.

Experimental procedures were performed in accordance with the National Institutes of Health Guide for Care and Use of Laboratory Animals (National Research Council, 1996 and 86/609/EEC). The study followed the international guidelines on the ethical use of animals and was approved by the local Ethical committee of the Karolinska Institute (N535/12).

The authors of this communication, Sh. Takeda, P. Mannström, S. Dash-Wagh, T. Yoshida, and M. Ulfendahl, confirm the absence of any conflict related to commercial or financial interests, to interrelations with organizations or persons in any way involved in the research, and to interrelations of the co-authors.

Ш. Такеда[1–3], П. Манстрьом[1], С. Деш-Ваг[1], Т. Йошида[2], М. Ульфендаль[1]

ВПЛИВИ СТАРІННЯ ТА ДІЇ ШУМУ НА СТОВБУРОВІ СЛУХОВІ ВІДПОВІДІ ТА КІЛЬКІСТЬ ПРЕСИНАПТИЧНИХ СТРІЧОК У КЛІТИНАХ ВНУТРІШНЬОГО ВУХА МИШЕЙ ЛІНІЇ C57BL/6J

[1]Каролінський інститут, Стокгольм (Швеція).
[2] Вища медична школа Університету Ехіме, Ехіме (Японія).
[3] Хірургічний отоларингологічний центр Оїкі, Осака (Японія).

Р е з ю м е

Втрата слуху розвивається у мишей лінії C57BL/6J у ранній період онтогенезу. Впливи старіння та дії шуму на кількість пресинаптичних структур у клітинах внутрішнього вуха таких мишей досі не вивчалися. Ми реєстрували динаміку стовбурових слухових відповідей (ССВ) у мишей даної лінії та оцінювали зміни пресинаптичних стрічок у клітинах внутрішнього вуха. Впливи старіння та дії шуму на слух мишей C57BL/6J були піддані багатобічній верифікації. Втрата слуху під дією сеансів шуму на мишей віком п'ять тижнів прогресивно посилювалася. Найпершою зміною було падіння амплітуди першої хвилі ССВ. У експериментальних тварин також спостерігалася втрата волоскових клітин та нейронів спірального ганглія. За допомогою імуногістохімічної методики та конфокальної мікроскопії високої розподільної здатності було виявлено зменшення числа CtBP2-позитивних структур у внутрішніх волоскових клітинах у зонах, відмінних від низькочастотного регіону слухового завитку. З іншого боку, вплив потужного шуму на стрічки в синапсах внутрішніх волоскових клітин спостерігався тільки у найбільш високочастотній зоні.

REFERENCES

1. B. Yueh, N. Shapiro, C. H. MacLean, and P. G. Shekelle, "Screening and management of adult hearing loss in primary care: scientific review," *J. Am. Med. Assoc.* **289**, 1976-1985 (2003).
2. F. R. Lin, R. Thorpe, S. Gordon-Salant, and L. Ferrucci, "Hearing loss prevalence and risk factors among older adults in the United States," *J. Gerontol. Biol. Sci. Med. Sci.,* **66**, 582-590 (2011).
3. S. G. Kujawa and M. C. Liberman, "Acceleration of age-related hearing loss by early noise exposure: evidence of a misspent youth," *J. Neurosci.* **26**, 2115-2123 (2006).

4. E. Daniel, “Noise and hearing loss: a review,” *J. School Health,* **77**, No. 5, 225-231 (2007).
5. D. O. Mikaelian, “Development and degeneration of hearing in the C57/b16 mouse: relation of electrophysiologic responses from the round window and cochlear nucleus to cochlear anatomy and behavioral responses,” *Laryngoscope,* **89**, 1-15 (1979).
6. K. R. Henry and R. A. Chole, “Genotypic differences in behavioral, physiological and anatomical expressions of age-related hearing loss in the laboratory mouse,” *Audiology*, **19**, 369-383 (1980).
7. J. F. Willott, J. Kulig, and T. Satterfield, “The acoustic startle response in DBA/2 and C57BL/6 mice: relationship to auditory neuronal response properties and hearing impairment,” *Hear. Res.,* **16**, 161-167 (1984).
8. J. F. Willott, “Effects of aging, hearing loss, and anatomical location on thresholds of inferior colliculus neurons in C57BL/6 and CBA mice,” *J. Neurophysiol.,* **56**, 391-408 (1986).
9. K. Parham and J. F. Willott, “Acoustic startle response in young and aging C57BL/6J and CBA/J mice,” *Behav. Neurosci.,* **102**, 881 (1988).
10. V. P. Spongr, D. G. Flood, R. D. Frisina, and R. J. Salvi, “Quantitative measures of hair cell loss in CBA and C57BL/6 mice throughout their life spans,” *J. Acoust. Soc. Am.,* **101**, 3546-3553 (1997).
11. R. R. Davis, J. K. Newlander, X. B. Ling, et al., “Genetic basis for susceptibility to noise-induced hearing loss in mice,” *Hear. Res.,* **155**, 82-90 (2001).
12. J. F. Willott, J. G. Turner, S. Carlson, et al., “The BALB/c mouse as an animal model for progressive sensorineural hearing loss,” *Hear. Res.,* **115**, 162-174 (1998).
13. L. C. Erway, J. F. Willott, J. R. Archer, and D. E. Harrison, “Genetics of age-related hearing loss in mice: I. Inbred and F1 hybrid strains,” *Hear. Res.,* **65**, 125-132 (1993).
14. K. Noben-Trauth, Q. Y. Zheng, and K. R. Johnson, “Association of cadherin 23 with polygenic inheritance and genetic modification of sensorineural hearing loss,” *Natl. Genet.,* **35**, 21-23 (2003).
15. J. Siemens, C. Lillo, R. A. Dumont, et al., “Cadherin 23 is a component of the tip link in hair-cell stereocilia,” *Nature,* **428**, 950-955 (2004).
16. S. P. Zachary and P. A. Fuchs, “Re-emergent inhibition of cochlear inner hair cells in a mouse model of hearing loss,” *J. Neurosci.*, **35**, No. 26, 9701-9706 (2015).
17. H. F. Schuknecht, *The Pathology of the Ear*, Harvard Univ. Press, Cambridge (1974).
18. H. S. Li and E. Borg, “Age-related loss of auditory sensitivity in two mouse genotypes,” *Acta Otolaryngol.,* **111**, 827-834 (1991).
19. S. Hequembourg and M. C. Liberman, “Spiral ligament pathology: a major aspect of age-related cochlear degeneration in C57BL/6 mice,” *J. Assoc. Res. Otolaryngol.,* **2**, 118-129 (2001).
20. M. C. Liberman, “Morphological differences among radial afferent fibers in the cat cochlea: an electron-microscopic study of serial sections,” *Hear. Res.,* **3**, 45-63 (1980).
21. Y. Sergeyenko, K. Lall, M. C. Liberman, and S. G. Kujawa, “Age-related cochlear synaptopathy: an early-onset contributor to auditory functional decline,” *J. Neurosci.,* **33**, 13686-13694 (2013).
22. A. C. Furman, S. G. Kujawa, and M. C. Liberman, “Noise-induced cochlear neuropathy is selective for fibers with low spontaneous rates,” *J. Neurophysiol.,* **110**, 577-586 (2013).
23. D. L. Newman, L. M. Fisher, J. Ohmen, et al., “GRM7 association with age-related hearing loss and its extension to additional features of presbycusis,” *Hear. Res.,* **294**, 125-132 (2012).
24. S. F. Maison, H. Usubuchi, and M. C. Liberman., “Efferent feedback minimizes cochlear neuropathy from moderate noise exposure,” *J. Neurosci.,* **33**, 5542-5552 (2013).
25. S. Stamataki, H. W. Francis, M. Lehar, et al., “Synaptic alterations at inner hair cells precede spiral ganglion cell loss in aging C57BL/6J mice,” *Hear. Res.,* **221**, 104-118 (2006).
26. H. J. G. Gundersen, “The nucleator,” *J. Microscop.,* **151**, 3-21 (1988).
27. A. Møller, P. Strange, and H. J. G. Gundersen, “Efficient estimation of cell volume and number using the nucleator and the disector,” *J. Microscop.,* 159, 61-71 (1990).
28. T. Tandrup, “A method for unbiased and efficient estimation of number and mean volume of specified neuron subtypes in rat dorsal root ganglion,” *J. Comp. Neurol.,* **329**, 269-276 (1993).
29. F. Watanabe, M. Kirkegaard, S. Matsumoto, et al., “Signaling through erbB receptors is a critical functional regulator in the mature cochlea,” *Eur. J. Neurosci.,* **32**, 717-724 (2010).
30. P. Mannström, B. Ulfhake, M. Kirkegaard, and M. Ulfendahl, “Dietary restriction reduces age-related degeneration of *stria vascularis* in the inner ear of the rat,” *Exp. Gerontol.,* **48**, 1173-1179 (2013).
31. H. J. G. Gundersen, T. F. Bendtsen, L. Korbo, et al., “Some new, simple and efficient stereological methods and their use in pathological research and diagnosis,” *Apmis,* **96**, 379-394 (1988).
32. H. J. G. Gundersen, P. Bagger, T. F. Bendtsen, et al., “The new stereological tools: disector, fractionator, nucleator and point sampled intercepts and their use in pathological research and diagnosis,” *Apmis,* **96**, 857-881 (1988).
33. H. C. Ou, G. W. Harding, and B. A. Bohne, “An anatomically based frequency–place map for the mouse cochlea,” *Hear. Res.,* **145**, 123-129 (2000).
34. A. Viberg and B. Canlon, “The guide to plotting a cochleogram,” *Hear. Res.,* **197**, 1-10 (2004).
35. J. F. Willott, J. VandenBosche, T. Shimizu, et al., “Effects of exposing C57BL/6J mice to high-and low-frequency augmented acoustic environments: Auditory brainstem response thresholds, cytocochleograms, anterior cochlear nucleus morphology and the role of gonadal hormones,” *Hear. Res.,* **235**, 60-71 (2008).
36. R. D. Frisina and X. Zhu, “Auditory sensitivity and the outer hair cell system in the CBA mouse model of age-related hearing loss,” *Open Access Anim. Physiol.,* **2**, 9-16 (2010).
37. J. S. Buchwald and C. H. Huang, “Far-field acoustic response: origins in the cat,” *Science,* **189**, 382-384 (1975).
38. S. G. Kujawa and M. C. Liberman, “Synaptopathy in the noise-exposed and aging cochlea: primary neural degeneration in acquired sensorineural hearing loss,” *Hear. Res.,* **330**, 191-199 (2015).
39. I. Tasaki, “The electrosaltatory transmission of the nerve impulse and the effect of narcosis upon the nerve fiber,” *Am. J. Physiol.,* **127**, 211-227 (1939).

40. N. Y. Kiang, M. C. Liberman, and R. A. Levine, "Auditory-nerve activity in cats exposed to ototoxic drugs and high-intensity sounds," *Ann. Otol. Rhinol. Laryngol.,* **85**, 752-768 (1976).
41. H. Spoendlin, "Factors inducing retrograde degeneration of the cochlear nerve," *Ann. Otol. Rhinol. Laryngol.,* Suppl*.,* **112**, 76-82 (1983).
42. G. M. Cohen, J. C. Park, and J. S. Grasso, "Comparison of demyelination and neural degeneration in spiral and Scarpa's ganglia of C57BL/6 mice," *J. Electron Microscop. Tech.,* **15**, 165-172 (1990).
43. T. Kurioka, M. Y. Lee, A. N. Heeringa, et al., "Selective hair cell ablation and noise exposure lead to different patterns of changes in the cochlea and the cochlear nucleus," *Neuroscience,* **332**, 242-257 (2016).
44. H. Spoendlin, "Innervation patterns in the organ of Corti of the cat," *Acta Otolaryngol.,* **67**, 239-254 (1969).
45. D. Robertson, "Functional significance of dendritic swelling after loud sounds in the guinea pig cochlea," *Hear. Res.,* **9**, 263-278 (1983).
46. M. C. Liberman and N. Y. Kiang, "Acoustic trauma in cats: cochlear pathology and auditory-nerve activity," *Acta Otolaryngol.,* **358**, 1-63 (1978).
47. A. M. Taberner and M. C. Liberman, "Response properties of single auditory nerve fibers in the mouse," *J. Neurophysiol.,* **93**, 557-569 (2005).
48. R. A. Schmiedt, J. H. Mills, and F. A. Boettcher, "Age-related loss of activity of auditory-nerve fibers," *J. Neurophysiol.,* **76**, 2799-2803 (1996).
49. S. G. Kujawa and M. C. Liberman, "Adding insult to injury: cochlear nerve degeneration after "temporary" noise-induced hearing loss," *J. Neurosci.,* **29**, 14077-14085 (2009).
50. J. Bourien, Y. Tang, C. Batrel, et al., "Contribution of auditory nerve fibers to compound action potential of the auditory nerve," *J. Neurophysiol.,* **112**, No. 5, 1025-1039 (2014).
51. H. W. Lin, A. C. Furman, S. G. Kujawa, and M. C. Liberman, "Primary neural degeneration in the Guinea pig cochlea after reversible noise-induced threshold shift," *J. Assoc. Res. Otolaryngol.,* **12**, 605-616 (2011).
52. K. K. Ohlemiller, J. M. Lett, and P. M. Gagnon, "Cellular correlates of age-related endocochlear potential reduction in a mouse model," *Hear. Res.,* **220**, 10-26 (2006).